International Journal of Astrobiology 5 (4): 295–306 (2006) Printed in the United Kingdom
doi:10.1017/S1473550406003478 First published online 26 November 2006

Potential of ozone formation by the smog mechanism to shield the surface of the early Earth from UV radiation

John Lee Grenfell[1]*, Barbara Stracke[1], Beate Patzer[2], Ruth Titz[1] and Heike Rauer[1]

[1]*Institut für Planetenforschung, Extrasolare Planeten und Atmosphären, Deutsches Zentrum für Luft- und Raumfahrt (DLR), Rutherford Str. 2, 12489 Berlin, Germany*
e-mail: lee.grenfell@dlr.de
[2]*Zentrum für Astronomie und Astrophysik, Technische Universität Berlin (TUB), Hardenbergstr. 36, 10623 Berlin, Germany*

Abstract: We propose that the photochemical smog mechanism produced substantial ozone (O_3) in the troposphere during the Proterozoic period, which contributed to ultraviolet (UV) radiation shielding, and hence favoured the establishment of life. The smog mechanism is well established and is associated with pollution hazes that sometimes cover modern cities. The mechanism proceeds via the oxidation of volatile organic compounds such as methane (CH_4) in the presence of UV radiation and nitrogen oxides (NO_x). It would have been particularly favoured during the Proterozoic period given the high levels of CH_4 (up to 1000 ppm) recently suggested. Proterozoic UV levels on the surface of the Earth were generally higher compared with today, which would also have favoured the mechanism. On the other hand, Proterozoic O_2 required in the final step of the smog mechanism to form O_3 was less abundant compared with present times. Furthermore, results are sensitive to Proterozoic NO_x concentrations, which are challenging to predict, since they depend on uncertain quantities such as NO_x source emissions and OH concentrations. We review NO_x sources during the Proterozoic period and apply a photochemical box model having methane oxidation with NO_x, HO_x and O_x chemistry to estimate the O_3 production from the smog mechanism. Runs suggest the smog mechanism during the Proterozoic period can produce approximately double the present-day ozone columns for NO_x levels of 1.53×10^{-9} by volume mixing ratio, which was attainable according to our NO_x source analysis, with 1% of the present atmospheric levels of O_2. Clearly, forming ozone in the troposphere is a trade-off for survivability – on the one hand, harmful UV radiation is blocked, but on the other hand ozone is a respiratory irratant, which becomes fatal at concentrations exceeding about 1 ppmv.

Received 3 June 2006, accepted 28 August 2006

Key words: early Earth, ozone, smog mechanism, UV-shielding.

Introduction

Understanding the atmospheric composition of the early Earth is linked to fundamental questions concerning the origin and establishment of life (e.g. Bada 2004). The chemistry of the early Earth's atmosphere is also highly relevant to forthcoming missions such as Darwin (Léger *et al.* 1996; Léger 2000) and NASA's Terrestrial Planet Finder (TPF) (Beichman *et al.* 1999) which will search for biomarker molecules on 'Earth-like' worlds, because many stars in the solar neighbourhood (closer than 30 pc) relevant to Darwin are younger than our Sun (Lammer *et al.* 2005).

Several ultraviolet-shielding (UV-shielding) mechanisms have been proposed to explain how living organisms managed to colonize the surface despite strong UV exposure in the early stages of the Earth's history. For example, Sagan & Chyba (1997) proposed UV-shielding from a fine, hydrocarbon haze, beneath which high levels of ammonia could accumulate. However, Pavlov *et al.* (2001) could not reproduce their result, instead calculating a much weaker shielding effect, attributed to differences in the aerosol size distribution. Selsis *et al.* (2002a) suggested some abiotic stratospheric ozone production and hence UV-shielding via carbon dioxide (CO_2) and water (H_2O) photolysis. Cleaves & Miller (1998) proposed that shielding was provided by an 'oil slick' of organic material which covered the early oceans. Thomas *et al.* (2004) investigated abiotic O_3 production and hence UV-shielding in a CO_2-rich atmosphere.

Similar to our work, Segura *et al.* (2003) considered O_2 and O_3 changes using a model including CH_4 oxidation extending to the troposphere. However, unlike this work, they did not calculate large tropospheric O_3 changes, presumably because they adopted lower NO_x abundances in

* Corresponding author.

their model[1]. Levine *et al.* (1979) studied the early Earth with a troposphere–stratosphere column model. They assumed 3 ppbv NO_x, which is comparable with our study. Kasting & Donahue (1980) suggested that 3 ppbv may be too high. Since then, additional NO_x sources, for example via cosmic rays (CRs), have been better quantified, as we will discuss. Also, the Levine study did not include CH_4 oxidation and was published before the recently proposed high CH_4 values, so the smog mechanism operated much more slowly in their model. In this study, we suggest a link between tropospheric O_3 formed from the smog mechanism, UV-shielding and the development of life on the early Earth.

We have performed sensitivity studies with a photochemical model investigating the atmospheric composition of the early Earth. We varied the initial concentrations of key species which can influence the smog mechanism (CH_4, O_2, NO_x, H_2, CO) within currently reported uncertainty limits. An overview of Proterozoic NO_x sources is provided and an ambient NO_x concentration is estimated for the early Earth. Finally, we estimate an overhead O_3 column produced via the smog mechanism, and discuss its potential to provide an UV shield for the early Earth and the implications for life.

The model

The smog mechanism and its chemical key species

The O_3 smog mechanism was first discussed in detail by Haagen-Smit (1951) who studied smog formation in Los Angeles. The mechanism requires a volatile organic compound (VOC) such as CH_4 and some NO_x in the presence of sunlight in order to form ozone, as illustrated below:

$CH_4 + OH \rightarrow CH_3 + H_2O$	(usually) rate determining, i.e. slowest step,
$CH_3 + O_2 + M \rightarrow CH_3O_2 + M$	fast formation of peroxy radical,
$NO + CH_3O_2 \rightarrow NO_2 + CH_3O$	peroxy radical gives up an O to NO,
$CH_3O + O_2 \rightarrow CH_2O + HO_2$	CH_3O rearranges to release HO_2,
$NO + HO_2 \rightarrow NO_2 + OH$	fast re-partitioning of HO_x and NO_x,
$NO_2 + h\nu \rightarrow NO + O$	fast photolysis of NO_2,
$O + O_2 + M \rightarrow O_3 + M$	three-body formation of ozone.

The mechanism begins with an attack of a hydroxyl (OH) radical upon a VOC such as methane to form an organic radical (R), for example CH_3 as shown above, plus water. Then, O_2 molecules quickly add on to R, to produce a peroxy radical (RO_2). This rapidly donates one of its O atoms to nitrogen monoxide (NO) to form nitrogen dioxide (NO_2) plus CH_3O. The CH_3O undergoes a re-arrangement reaction and expels HO_2. The HO_2 quickly donates an O to NO, forming NO_2. The NO_2 quickly photolyses to reform the original NO plus O. The latter reacts with O_2 to form O_3. The smog mechanism has been confirmed by numerous modelling and theoretical studies (e.g. Demerjian *et al.* 1974; Kumar & Mohan 2002).

Enhanced UV radiation in the lower atmosphere during the Proterozoic period clearly favours the smog mechanism. But how much more surface UV radiation would we expect without an O_3 shield? Modern-day surface UV-B radiation on Antarctica increases by a factor of three to six in September/October (Stamnes *et al.* 1992) when up to half the overhead O_3 is destroyed as a result of the 'O_3 hole'. Segura *et al.* (2003) reported that modelled surface UV-B radiation increases by a factor of 11 for abiotic ($O_2 = 10^{-5}$ present atmospheric levels (PAL)) conditions. Clearly the abiotic atmosphere may have seen very harsh surface UV levels, despite the fainter sun, unless of course there featured a non-O_3 UV shield.

High CH_4 concentrations during the Proterozoic period would clearly favour the smog mechanism. Evidence for high Proterozoic CH_4 is linked with the 'faint young Sun paradox'. The early Sun showed a weaker flux in the UV/visible range. This evoked high levels of greenhouse gases in the atmosphere, explaining why liquid H_2O existed on the early Earth, as suggested by the geologic record (e.g. Sagan & Mullen 1972). Kasting (1993), for example, suggested high Proterozoic levels of CO_2 to explain the paradox. Paleosol data (Rye *et al.* 1995), however, did not subsequently support such levels. Pavlov *et al.* (2000) then suggested that the paradox provides indirect evidence for high Proterozoic CH_4. Pavlov *et al.* (2000, 2003) suggested $(1.0–3.0) \times 10^{-4}$ vmr CH_4 and Selsis (2000) implied an upper limit of 1×10^{-3} vmr. Such high values arose from low hydroxyl concentrations, an important sink for CH_4 during the Proterozoic period. OH concentration was low because it was consumed by high levels of Proterozoic CO and H_2 (Brown 1999).

High CO levels from CO_2 photolysis could build up during the Archaean period. Kasting & Catling (2003) suggested 5.5×10^{-3} vmr. This would also favour the smog mechanism – here, an analagous series of O_3-forming reactions occur but with CO replacing CH_4. However, Proterozoic CO is not well determined. Part of the uncertainty arises from opposing effects, as discussed in Pavlov & Kasting (2002). On the one hand, during the *early* Proterozoic period, O_2 and O_3 concentrations were very low which meant that high levels of UV flux reached the surface and were able to photolyse water vapour to produce OH. As O_2 levels increased further this effect weakened, leading to decreased OH levels (and hence increased CO and H_2). On the other hand, during the mid to late Proterozoic period (see Fig. 1), there existed an opposing mechanism, which increased OH levels. Here, rising O_2 (and hence O_3) levels lead to increased OH levels (hence decreased CO and H_2) via $O_3 + h\nu \rightarrow O_2 + O(^1D)$, then $O(^1D) + H_2O \rightarrow 2OH$. In our runs, we adopted a factor of 10 *decrease* for Proterozoic CO levels compared with Archaean values, corresponding to the mechanism operating in the mid

[1] They assumed 21 pptv NO_x at the surface and 159 pptv NO_x in the mid troposphere.

https://doi.org/10.1017/S1473550406003478 Published online by Cambridge University Press

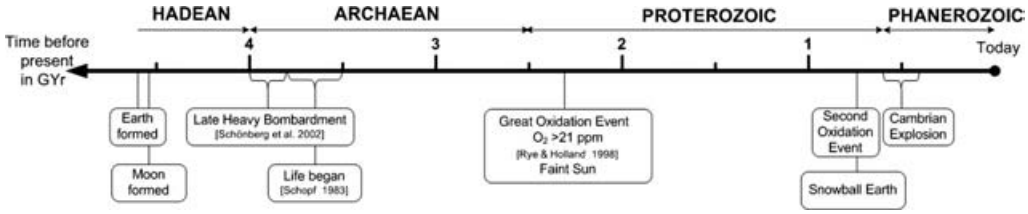

Fig. 1. Geological timescale in 1×10^9 yr (Gyr) summarizing the development of the Earth's atmosphere. The various geological periods or 'eons' are shown in capitals. Important events which influenced the atmosphere are shown in boxes.

to late Proterozoic period. However, model tests suggest that the uncertainty in this compound does not greatly affect the conclusions – the O_3 column was far more sensitive to changes in CH_4 and NO_x.

H_2O indirectly affects the smog mechanism, because it photolyses to produce HO_x ($=OH+HO_2$), which removes NO_x ($=NO+NO_2$) into inactive, reservoir forms, for example $OH+NO_2+M \rightarrow HNO_3$ (nitric acid)$+M$ or via $OH+NO+M \rightarrow HONO$ (nitrous acid)$+M$. 'M' represents any available species (typically N_2) required to carry away excess energy from the reaction which would otherwise cause the products to fall apart immediately. Surface H_2O levels in our model was set to vary sinusoidally in all runs from $(1.0–1.3) \times 10^{-2}$ vmr from midnight to midday, respectively, consistent with the results of Kasting (1997) and Kasting & Catling (2003). H_2 indirectly affects the smog mechanism by shifting the OH/HO_2 ratio to favour HO_2. Kasting & Catling (2003) suggested a value of Archaean H_2 of 1×10^{-3} vmr. This value was derived by balancing volcanic emissions with loss rates via escape to space. Tian *et al.* (2005) recently argued that loss to space may have occurred up to 100 times slower than previously thought, which would imply a much higher value for Archaean H_2 of up to 0.3 vmr. In our runs we adopted a factor of 10 decrease for the level of Proterozoic H_2 compared with the Archaean value from Kasting & Catling (2003).

O_2 is required by the smog mechanism to form O_3 via $O+O_2+M \rightarrow O_3+M$. Kasting & Catling (2003) provide a review on the rise of atmospheric O_2. Sulphur isotope data (Farquhar *et al.* 2001; Pavlov & Kasting 2002) and trace sulphate data (Hurtgen *et al.* 2002) suggest that O_2 concentrations rose to at least 21 ppmv 2.3 billion years ago (Ga), a rise termed the 'Great Oxidation Event' (GOE) and believed to be associated with cyanobacteria. The GOE may have been favoured by high methane levels because methane can diffuse into the upper atmosphere where it photolyses and subsequently loses some of its hydrogen, which is a strong sink for O_2, to space (Kerr 2005). O_2 levels then rose again, i.e. the 'Second Oxidation Event' (SOE), between 0.6 and 0.8 Ga. Many scientists contend that the SOE was related to an increase in the removal rate of organic carbon, which otherwise rapidly consumes O_2 into sediment, but the exact mechanism is not clear (Kerr 2005). Lenton *et al.* (2004) suggested that the SOE was linked with increased weathering of rocks which led to more phosphorous (a nutrient) being released into the seas, favouring more O_2 production. The increased weathering may have been due to the formation of a supercontinent and/or the arrival of lichens on land (Kerr 2005). Typical 'background' O_2 Archaean values are 10^{-14} to 10^{-18} vmr, usually quoted based on model output (Kasting 1993) with Proterozoic values typically varying between 0.1 and 10% present-day O_2 levels.

NO_x is required to catalyse the O_3 smog mechanism. In today's atmosphere, about 50×10^{12} g yr^{-1} (or 50 Tg yr^{-1}) of nitrogen are emitted into the atmosphere in the form of NO_x (Houghton *et al.* 2001), 60% comes from industry and most of the remainder comes from soils, lightning and biomass burning. Typical modern-day NO_x concentrations vary from about 10 pptv in very clean air, up to 100 ppbv in very polluted air. In the abiotic atmosphere NO_x could have built up to 1 ppmv from natural sources (Selsis *et al.* 2002b) because levels of OH, an important NO_x sink, were low. Navarro-González *et al.* (2001) suggested a NO_x source of 1–10 Tg N yr^{-1} (terragrams of nitrogen per year) in the abiotic atmosphere based on simulated lightning-discharge experiments. CRs associated with an active sun may lead to N_2 dissociation and hence NO_x formation in the middle atmosphere at high latitudes (Callis *et al.* 2001; Randall *et al.* 2001). Recent model studies (e.g. Langematz *et al.* 2005) suggest a potentially large effect, i.e. NO_x changes in excess of 10 ppbv, despite large uncertainties. In the early Earth, this effect may have been even larger because the high energy output of the Sun (X-ray, Solar wind density) was up to 100–1000 times higher than that of the present day (Guinan & Ribas 2002; Ribas *et al.* 2005). Smith *et al.* (2004) investigated the effects of ionizing radiation (e.g. stellar flares, galactic CRs, energetic particles) in terrestrial-like exoplanets from a radiative standpoint, but without considering NO_x formation mechanisms.

To decide the level of NO_x to be set in our study, Table 1 gives an overview of NO_x sources for the early Earth's atmosphere and the pre-industrial atmosphere (*circa* 1850). Perhaps most interesting is the CR mechanism. Uncertainties here are large, but the CR source strength is also potentially very large, because extreme UV enhancement factors for the early Earth of 100 have been suggested (Guinan & Ribas 2002). In today's atmosphere, CR produce NO_x *in situ* in the middle atmosphere polewards of 60°. Model studies (Rozanov *et al.* 2004; Langematz *et al.* 2005) suggest that a significant NO_x signal can then spread to lower altitudes and latitudes. For the early Earth, we assumed a NO_x soil source varying from present-day levels up to double the present-day

https://doi.org/10.1017/S1473550406003478 Published online by Cambridge University Press

Table 1. *Comparison of pre-industrial NO_x sources with those of the early Earth. Unless otherwise stated, units are teragrammes nitrogen per year ($Tg\ N\ yr^{-1}$). E is the extreme UV factor*

Mechanism	Reference	Pre-industrial value	Assumed Proterozoic value
Thunderstorm lightning	Price & Rind (1994) Navarro-González *et al.* (2001)	1.0–12.0	1.0–10.0
Volcanic lightning	Mvondo *et al.* (2001)	Low	1.0–10.0
CRs	Rozanov *et al.* (2004) Langematz *et al.* (2005)	3–20 ppbv increase in the middle atmosphere	(3–20) × *E* ppbv
Soil microbes	Yienger & Levy (1996)	5.5	5.5–11.0

values. To estimate the ambient NO_x concentrations from the sources in Table 1, first we sum the various sources in Table 1 ignoring the uncertain CR source:

$$\text{sum pre-industrial } NO_x \text{ sources in Table 1} = (6.5-17.5)\ \text{Tg N yr}^{-1},$$
$$\text{sum early Earth } NO_x \text{ sources in Table 1} = (7.5-31.0)\ \text{Tg N yr}^{-1},$$
$$NO_x \text{ factor (early Earth/pre-industrial)} = (7.5-31.0)/(6.5-17.5) = (0.43-4.77).$$

The pre-industrial general circulation model (GCM) study of Grenfell *et al.* (2001) without CRs suggested an ambient pre-industrial NO_x concentration of 0.32 ppbv. Therefore, we assume:

$$\text{early Earth } NO_x \text{ concentration} = \text{pre-industrial } NO_x \text{ concentration} \times NO_x \text{ factor} = 0.32\ \text{ppbv} \times (0.43-4.77) = (0.14-1.53)\ \text{ppbv}.$$

Based on the above, we performed sensitivity runs with NO_x set to 0.14 and 1.53 ppbv.

The above analysis does not consider changes in levels of OH between the present day and the early Earth. However, early Earth OH levels are uncertain and subject to the opposing mechanism as discussed earlier.

We also performed runs with NO_x set to 20 ppbv. This represents an upper limit for the CR mechanism and assumes that NO_x produced by this mechanism in the mid to upper atmosphere at high latitudes is able to penetrate into the troposphere. The extent to which this occurs is currently a focus of research for the Earth modelling community; for example, Sinnhuber *et al.* (2003) suggested that 10–20 ppbv NO_x could reach at least down to 20 km whereas Quack *et al.* (2001) suggested that such values remained above 40 km.

An interesting point is that levels of NO_x, and therefore also ozone, on the early Earth would clearly have been enhanced close to its sources, for example massive volcanoes that generated their own lightning. Therefore, even if NO_x could not build up globally because it was destroyed by high OH levels, nevertheless individual 'islands' of NO_x with associated ozone could have survived close to NO_x sources. We envisage that these would have offered at least isolated pockets of shielding from UV and hence encouraged the establishment of life in a heterogeneous manner. We quantify these ideas in the 'Results' section.

Computational details

Our approach is somewhat different to other modelling studies of the early Earth (e.g. Kasting 1993; Segura *et al.* 2003). Those studies typically employed column models integrated until specified emission rates of source gases reach equilibrium with their sinks. Photolysis rates in those studies were diurnally averaged. Our model takes the approach of a box model, as used in modern-day atmospheric chemistry measurement campaigns. It solves a chemical reaction network for a particular location and time with assumed source gas concentrations, temperature, humidity, pressure, etc. Then, important reactive intermediates such as O_3 and OH are calculated including diurnal variations. In this work, we vary source gases (O_2, H_2, CO, CH_4 and NO_2) within reasonable bounds of uncertainty for the early Earth, then use our model to calculate the reactive intermediates. The advantages of the box model approach are:

- the accurately validated output compares well with present-day observations;
- attributing chemical responses between runs is relatively straightforward;
- the model requires a short integration time for the reactive intermediates to adjust to the specified source gas concentrations; and hence
- a large number of sensitivity runs may be performed.

These calculations can also act as a basis for a column model developed in the future.

We used the FACSIMILE commercial integrating package developed by the Materials and Chemical Process Assessment (MCPA). Chemical reactions were treated as a system of non-linear, time-dependent differential equations and solved using the Gear method (Gear *et al.* (1985) and references therein). Our straightforward tropospheric chemical scheme featured inorganic HO_x, NO_x and O_x reactions and comprised 55 photochemical reactions for 25 species, ten of which were photolysis reactions, including CH_4 oxidation. The basic scheme is available at http://mcm.leeds.ac.uk/MCM. The full set of equations solved here is given in Appendix A.

https://doi.org/10.1017/S1473550406003478 Published online by Cambridge University Press

We ran for perpetual[2] June conditions at a latitude of 53° N, corresponding to the atmospheric measurement station at Weybourne in England. This latitude was originally chosen for present Earth model validation. In the absence of Proterozoic data, the temperature in the model varied sinusoidally from 290 to 298 K from midnight to midday, respectively, and relative humidity varied from 44 to 90% from midnight to midday, respectively.

Photolysis rates (J) were of the form $J = K\cos(sza)^{L}\exp(-M\sec(sza))$ where K, L, M are molecule-dependent constants and sza = solar zenith angle. These expressions were derived from previous runs of a GCM, as described in Hough (1988). The model included a parameterization to calculate mixing height (H) using a time-dependant triangular spike function that varied from 300 m at midnight to 1300 m at midday. The variation reflects the heating of the surface during the daytime, leading to convective currents pushing the mixing height upwards. Calculating the mixing height was important because it determined the rate of loss of species to the ground. This was parameterized via the so-called deposition velocities (D (cm s^{-1})). Physically, these represent the 'stickiness' of a species, i.e. how quickly it may travel to the surface and be permanently removed there. Numerically, the rate of loss via deposition in the model, $k_{dep} = (D/H)\ s^{-1}$, where

$D(HNO_3) = 2.0$ cm s^{-1},
$D(NO_2) = 0.15$ cm s^{-1},
$D(O_3) = 0.5$ cm s^{-1},
$D(H_2O_2) = 1.1$ cm s^{-1},
$D(HCHO)$ (formaldehyde) $= 0.33$ cm s^{-1},
$D(CH_3NO_3) = 1.1$ cm s^{-1},
$D(CH_3OOH) = 0.55$ cm s^{-1}.

Photolysis rates for the early Earth ($J_{\text{early Earth}}$) were calculated for a particular species via

$$J_{\text{early Earth}} = J \times F \times C$$

where J represents present-day photolysis rates, F is the faint Sun factor and C is a factor depending on the overhead ozone column. Numerically, $F = (1 + 0.4(1 - t/t_0))^{-1}$ where t_0 is the present age of the Earth (= 4.6 Gyr), and t is the age of the early Earth (in Gyr). For our runs we took t to be 3.9 Gyr, i.e. around the time of the second oxidation event (see Fig. 1). This resulted in an F-value of 0.943. The column factor, C, represents increases in ground UV radiation due to a weaker stratospheric O_3 column for the early Earth. We derived C-values from Segura *et al.* (2003) who performed calculations with, for example, 1 and 10% O_2 using a column model. Those authors split C-factor contributions into their UV-A, UV-B and UV-C components (see table 2 of Segura *et al.* (2003)). In order to be consistent with the Segura C-values, we also split photolysis processes in our model into contributions from UV-A, UV-B and UV-C radiation, as shown in Table 2.

[2] Solar zenith and local hour angles are calculated based on mean June conditions, and hence the length and amplitude of the diurnal cycle in flux is constant from day to day.

Table 2. *Contribution of the photolysis rate to a particular wavelength region (in the UV-A, UV-B and UV-C). Values represent the product ($\sigma \times \phi$) for a particular species, where σ = absorption cross-section, ϕ = quantum yield, shown as the percentage contribution over the entire (UV-A, UV-B and UV-C) range. Source*: *DeMore et al. (1994) (to be consistent with FACSIMILE)*

Photolysis reaction	Percentage UV-A (315–400 nm)	Percentage UV-B (280–315 nm)	Percentage UV-C (200–280 nm)
$CH_3NO_3 \rightarrow CH_3O + NO_2$	1.4	51.8	46.8
$CH_3OOH \rightarrow CH_3O + OH$	0.6	3.3	96.1
$H_2O_2 \rightarrow 2OH$	0.3	1.9	97.8
$HNO_3 \rightarrow OH + NO_2$	0	0.1	99.9
$HONO \rightarrow OH + NO$	0.2	10.5	89.3
$NO_2 \rightarrow NO + O$	67.3	6.9	25.8
$O_3 \rightarrow O_2 + O(^1D)$	0	7.1	92.9
$O_3 \rightarrow O_2 + O(^3P)$	0.5	4.7	94.8

Table 3. *Overview of source gas concentrations in the 36 sensitivity runs*

Run number					
1% O_2	10% O_2	H_2	CO	CH_4	NO_2
1	19	1×10^{-4}	5.5×10^{-6}	1.0×10^{-4}	0.14×10^{-9}
2	20	1×10^{-3}	5.5×10^{-6}	1.0×10^{-4}	0.14×10^{-9}
3	21	5×10^{-7}	5.5×10^{-6}	1.0×10^{-4}	0.14×10^{-9}
4	22	1×10^{-4}	5.5×10^{-5}	1.0×10^{-4}	0.14×10^{-9}
5	23	1×10^{-4}	2.7×10^{-8}	1.0×10^{-4}	0.14×10^{-9}
6	24	1×10^{-4}	5.5×10^{-6}	3.0×10^{-4}	0.14×10^{-9}
7	25	1×10^{-4}	5.5×10^{-6}	1.0×10^{-4}	1.53×10^{-9}
8	26	1×10^{-3}	5.5×10^{-6}	1.0×10^{-4}	1.53×10^{-9}
9	27	5×10^{-7}	5.5×10^{-6}	1.0×10^{-4}	1.53×10^{-9}
10	28	1×10^{-4}	5.5×10^{-5}	1.0×10^{-4}	1.53×10^{-9}
11	29	1×10^{-4}	2.7×10^{-8}	1.0×10^{-4}	1.53×10^{-9}
12	30	1×10^{-4}	5.5×10^{-6}	3.0×10^{-4}	1.53×10^{-9}
13	31	1×10^{-4}	5.5×10^{-6}	1.0×10^{-4}	20.0×10^{-9}
14	32	1×10^{-3}	5.5×10^{-6}	1.0×10^{-4}	20.0×10^{-9}
15	33	5×10^{-7}	5.5×10^{-6}	1.0×10^{-4}	20.0×10^{-9}
16	34	1×10^{-4}	5.5×10^{-5}	1.0×10^{-4}	20.0×10^{-9}
17	35	1×10^{-4}	2.7×10^{-8}	1.0×10^{-4}	20.0×10^{-9}
18	36	1×10^{-4}	5.5×10^{-6}	3.0×10^{-4}	20.0×10^{-9}

In total, 36 sensitivity runs were performed, as summarized in Table 3. The fixed species in the model were varied from run to run to represent uncertainties in their concentrations (refer to the previous section). The response time is relatively short because the long-term source gases in the model are specified by the user. The model runs reached equilibrium after about 10–20 days. However, the model sometimes experienced numerical problems whereby the integrator failed to converge. This usually occurred at dawn and/or dusk when chemical concentrations changed rapidly and drastically. The problem affected the 1% PAL O_2 runs since these

https://doi.org/10.1017/S1473550406003478 Published online by Cambridge University Press

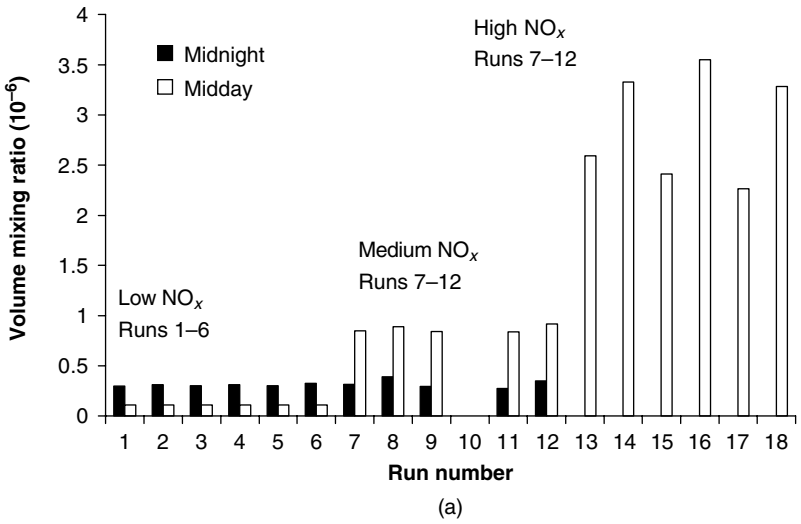

Fig. 2. (a) Surface ozone concentration in mixing ratio (1×10^{-6}) for O_2 (runs 1–18) set to 1% PAL during the Proterozoic era. Midnight values of converged runs are shown in black, midday in white. (b) As for (a) but for 10% PAL O_2 (runs 19–36).

represented the weakest ozone cover, and therefore featured the highest surface photolysis fluxes (see Figs 2(a) and 3(a)). The convergence problem also occurred at night. This could mean that the constraints we imposed, i.e. constant NO_x, CH_4, CO, etc. are unrealistic, or it could indicate some missing night-time chemistry of the early Earth. Only calculations that reached equilibrium were included in Figs 2 and 3.

Results

Ozone

Figures 2(a) and 2(b) show the surface concentrations of ozone for 1 and 10% PAL O_2, respectively. Some midnight data are missing because the model sometimes featured convergence problems during the night, as already discussed. The values shown are all much enhanced compared with our pre-industrial control run, which featured midday $[O_3] = 2.8 \times 10^{-9}$ mixing ratio. Results in Figs 2(a) and 2(b) may be broadly split into three categories, namely low, medium and high ozone, which correspond to low (=0.14 ppbv), medium (=1.53 ppbv) and high (=20 ppbv) NO_x. The results suggest for the low and medium NO_x cases that ozone was controlled mainly by changes in NO_x rather than changes in CH_4, H_2 or CO. This is analagous to the present-day situation in many unpolluted regions of the Earth, which are said to be under 'NO_x control' with regards to ozone smog production (e.g. Shindell *et al.* 2001). For the high NO_x runs, however, ozone production appears to become 'saturated' with respect to NO_x and responds instead to changes in H_2, CO and CH_4. This is analagous to the situation today in some large cities which are said to be

https://doi.org/10.1017/S1473550406003478 Published online by Cambridge University Press

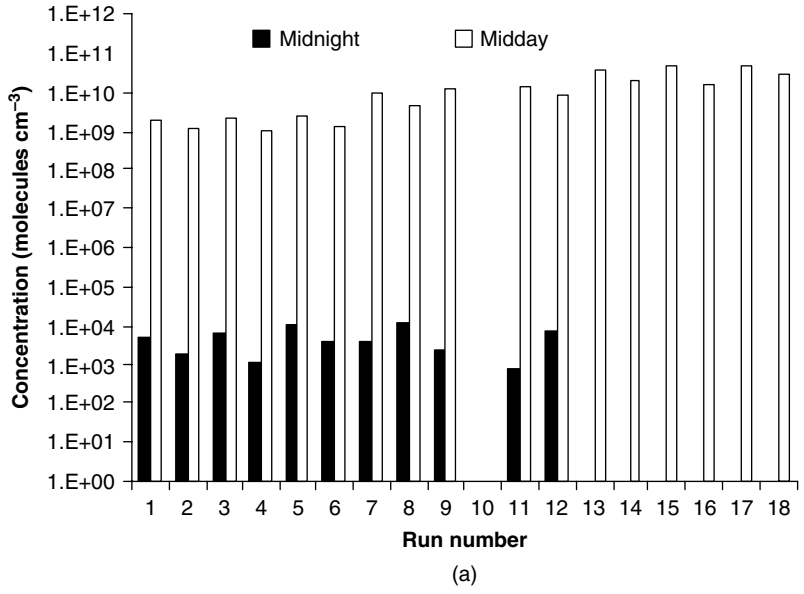

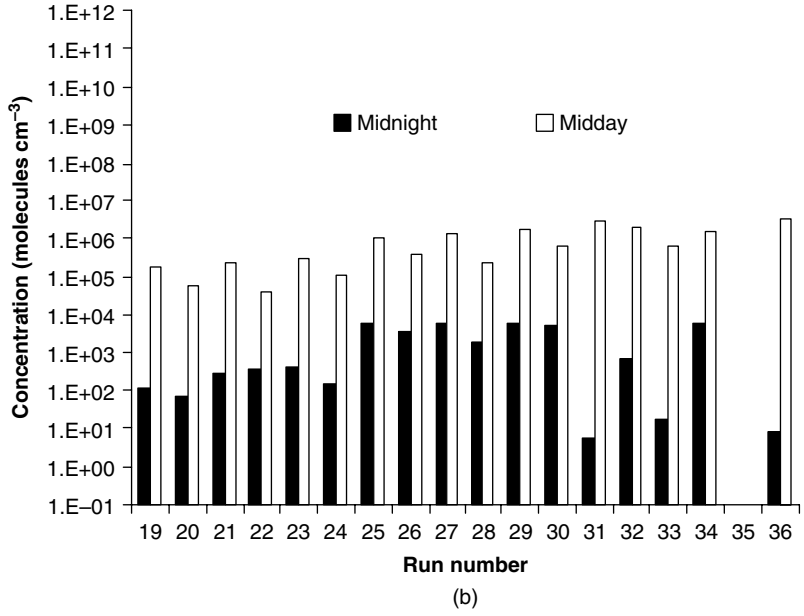

Fig. 3. (a) Surface OH concentration in molecules cm^{-3} for O_2 (runs 1–18) set to 1% PAL during the Proterozoic era. Midnight values of converged runs are shown in black, midday in white. (b) As for (a) but for 10% PAL O_2 (runs 19–36).

under 'hydrocarbon control' with regard to ozone smog production. For the high NO_x runs, increasing H_2, CO and CH_4 one by one by the amounts shown in Table 3 lead to an increase in midday O_3 from about 2.4 to 3.6 ppmv for the 1% PAL O_2 runs (Fig. 2(a)) and from 0.02 to 0.36 ppmv at midday for the 10% PAL O_2 runs (Fig. 2(b)).

Appendix B shows how we calculated the ozone column in Dobson Units (DU) using run 9 as an example (i.e. having medium levels of NO_x and VOCs). We assume a 12 km troposphere with constant ozone values as calculated by our box model for the surface. The calculation implies 564.3 DU for the troposphere of the early Earth, i.e. well in excess of today's total (tropospheric + stratospheric) ozone column of 300–350 DU.

Hydroxyl (OH)

Figures 3(a) and 3(b) are the same as Figs 2(a) and 2(b) but show hydroxyl. Our pre-industrial control run featured midday [OH] = 3.34×10^6 molecules cm^{-3}, i.e. the 1% PAL O_2 runs were enhanced by approximately a factor of 1000 compared with the control run although OH for the 10% PAL of O_2 runs was suppressed. We interpret this as follows: on the one hand, higher fluxes favour more OH although, on the other hand, less O_2 favours less OH compared with the control run. For the 1% PAL O_2 runs, it would seem that high fluxes lead to more OH, but for the 10% PAL O_2 runs, less O_2 leads overall to less OH compared with the control run.

https://doi.org/10.1017/S1473550406003478 Published online by Cambridge University Press

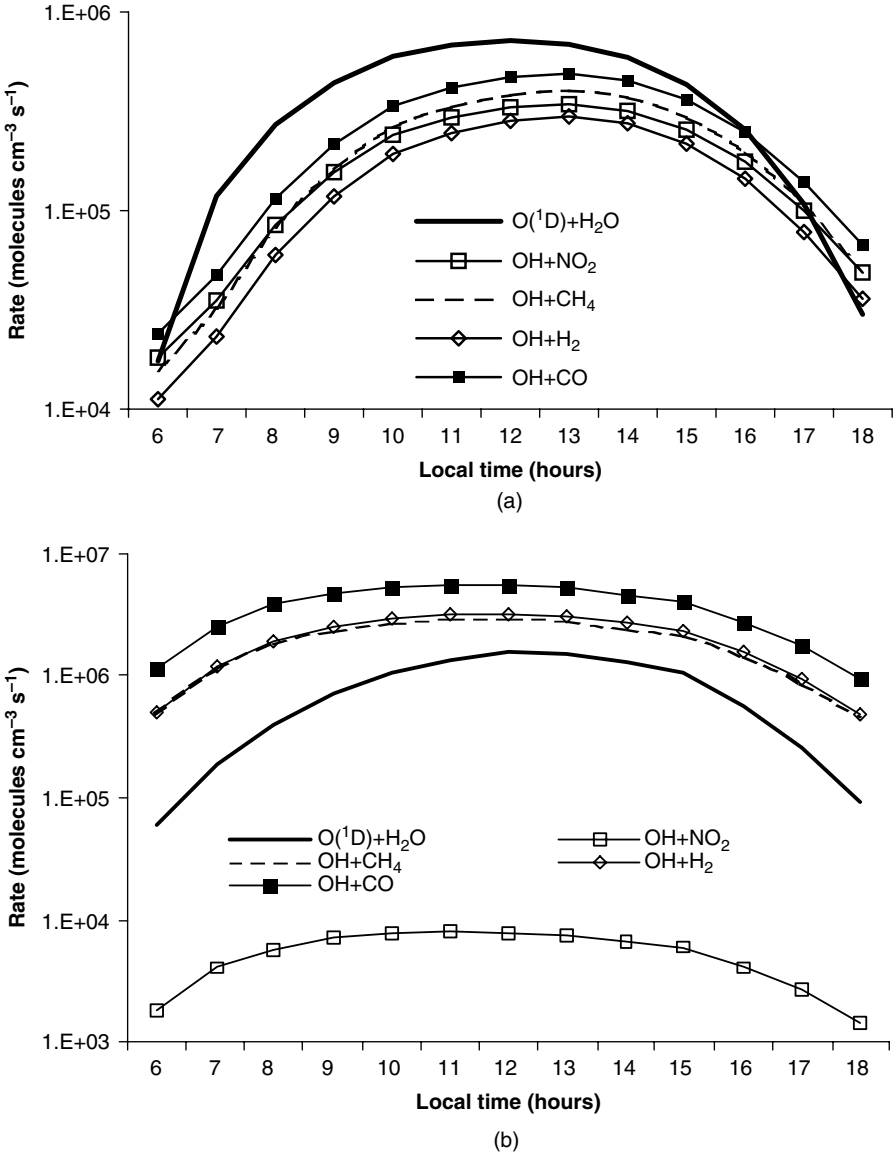

Fig. 4. (a) Major sources and sinks affecting OH in molecules cm^{-3} s^{-1} for the control run output hourly on the last day of the run. The source shown is $O(^1D)+H_2O \rightarrow 2OH$ (continuous line) and the four sinks: $OH+NO_2+M \rightarrow HNO_3+M$ (open squares), $OH+CH_4 \rightarrow CH_3+H_2O$ (dashed line), $OH+H_2+O_2 \rightarrow HO_2+H_2O$ (open diamonds) and $CO+OH \rightarrow CO_2+H$ (filled squares). (b) As for (a) but for the early Earth (run 19). This run features mean Proterozoic conditions, i.e. the long-lived source gases in the middle of their estimated ranges.

OH concentrations for a particular time of day exhibited minimal variation in the model after a relaxation period of about 5 days. In Figs 3(a) and 3(b), increasing CO, CH_4 or H_2 concentrations lead to a lowering in OH levels by a factor of 3–7. This is the expected result, since these compounds react directly with OH. Also, in both figures we see a slight upward trend with increasing run number at midday, i.e. with increasing NO_x levels. This effect has been studied (Prather *et al.* 2003) and arises via $HO_2+NO \rightarrow OH+NO_2$, i.e. as NO_x levels increase, HO_2 repartitions leading to an increase in OH. The upward trend is less clear for the midnight values especially for the case of high levels of NO_x, which could point to other processes playing a role; for example, at high NO_x levels, NO_2 becomes a *sink* for OH via $OH+NO_2+M \rightarrow HNO_3+M$, although the lack of data at midnight in Fig. 3(a) makes interpretation difficult.

Figures 4(a) and 4(b) show the rates of the major sinks CH_4+OH, NO_2+OH, H_2+OH, NO_2+OH and the major source for OH ($O(^1D)+H_2O \rightarrow 2OH$) for the control run and for a 'typical' early Earth run[3]. For the control run, the source $O(^1D)+H_2O$ proceeds faster than the sinks, which all proceed at an approximately comparable rate. For the early Earth run, the CO, CH_4 and H_2 sinks are all important – clearly any of these three could be the major remover of OH within their reported uncertainty range.

[3] In this case run 19, in which $(O_2)=10\%$ PAL and the long-lived source gases are in the mid-range of their reported values.

https://doi.org/10.1017/S1473550406003478 Published online by Cambridge University Press

Discussion

Ozone

The 1% PAL O_2 runs in Fig. 2(a) featured much higher daytime ozone levels (0.1–3.6 ppmv) compared with the 10% PAL O_2 runs in Fig. 2(b) (0.004–0.36 ppmv). This was associated with enhanced photolytic fluxes in the 1% PAL O_2 runs due to a weaker assumed overhead ozone column, which was coded into the model via the 'column factors' taken from the Segura study. The fact that stronger photolysis fluxes stimulate the ozone smog mechanism is widely accepted – ozone smog is a much greater problem in sunny cities such as Athens and Los Angeles, with increased flux leading to more ozone smog as already discussed.

Levels of midnight ozone for the 1% PAL O_2 runs is higher than its midday counterpart (Fig. 2(a)) for low NO_x levels (runs 1–6). In today's atmosphere, important mechanisms affecting nocturnal O_3 near the surface are (1) dry deposition of O_3 to the ground and (2) chemical removal of O_3 via $NO + O_3 \rightarrow NO_2 + O_2$. Regarding (1), the rate of dry deposition of ozone equals $k_{dep}(O_3)$, as already discussed in the 'Computational details' section. The 1% PAL O_2 runs featured higher O_3 levels and hence also *faster loss* to the ground compared with the 10% PAL O_2 runs, so clearly mechanism (1) cannot lead to higher midnight O_3 values in the 1% PAL O_2 case. Further checking revealed that mechanism (2) also could not explain the high midnight O_3 levels for the 1% PAL O_2 runs either. In fact, the 1% PAL O_2 runs featured a higher midnight NO level than the 10% PAL O_2 runs, which would imply less O_3. The higher NO level was related to a lower midnight OH level for the 1% PAL O_2 case, and hence slower removal of NO into its sinks. The lower midnight OH level was in turn related to the stronger daytime oxidation of methane in the case of the high flux 1% PAL O_2 run leading to higher concentrations of methane oxidation products such as HCHO and CH_3OOH, which perturbed the night chemistry and acted as sinks for OH.

To understand why midnight O_3 levels were higher in the 1% PAL O_2 runs 1–6, it was helpful to consider ozone concentrations over the diurnal cycle. In both the 1% PAL O_2 and 10% PAL O_2 cases there occurred an O_3 peak in the afternoon. This arose because typical response timescales of the smog cycle were a couple of hours, which led to O_3 levels lagging the midday peak in Solar intensity. However, the 1% PAL O_2 runs feature stronger daytime fluxes. This led to higher ozone levels at dusk which persisted until midnight, and hence the high midnight values of run 1–6.

Increasing NO_x levels from the medium to the high case (Figs 2(a) and (b)) lead to a rise in ozone by a factor of 2–3. Why? At high NO_x levels, the smog mechanism appears to become saturated and an opposing mechanism can play a role in which ozone is directly removed via NO. This behaviour is sometimes also seen in the centres of large cities, where NO is high owing to dense traffic but where ozone levels can be actually lower than in the suburbs. This low ozone effect is suggested by run 33.

Changing CO, CH_4 and H_2 concentrations had a much smaller effect on ozone compared with the NO_x concentration changes. For the low levels NO_x case, changing these three compound concentrations (Figs 2(a) and 2(b)) had only a very small effect on the ozone concentration.

For the medium level NO_x case, CO and CH_4 concentration changes typically resulted in small ozone volume mixing ratio changes of $(2–5) \times 10^{-8}$. Increasing H_2 levels by a factor of 10 (runs 7, 8, 25 and 26) led to an ozone concentration increase of 0.05×10^{-6}. Why? In the model, there is only one chemical reaction involving H_2, namely $OH + H_2 + O_2 \rightarrow HO_2 + H_2O$. So, H_2 can affect the HO_x (and hence NO_x) partitioning hence affect ozone, although the effect is small. The important point is that the overall effect of increasing H_2 levels leads to a small ozone concentration increase in the model.

For the high level NO_x runs, changing CO, CH_4 and H_2 concentrations lead to significant changes in ozone (Figs 2(a), 2(b)). For the 1% PAL O_2 runs (Fig. 2(a)) changing these three compound concentrations individually lead to ozone varying between 2.2×10^{-6} and 3.6×10^{-6}. More CH_4 and CO we simply interpret as leading to a faster smog mechanism and hence more ozone. For the high level NO_x runs the H_2 effect already discussed for the medium case runs is now stronger. Here, increasing H_2 levels from modern-day values to Proterozoic values leads to large increases in ozone, from about 0.030 ppm in run 33 to 0.36 ppm in run 34 (Figs 2(a) and 2(b)).

Hydroxyl

The OH values in Figs 3(a) and 3(b) can be used to constrain the NO_x lifetime in the early Earth, and hence estimate the size of the proposed UV 'protective pockets' in the vicinity of natural NO_x sources. Assume for the 1% PAL O_2 runs that the early Earth OH level is 1000 times higher than today's value. This is implied by Fig. 3(a) which shows a peak OH concentrations of about 1×10^9 molecules cm^{-1} whereas the typical modern-day peak is approximately 1×10^6 molecules cm^{-1}, i.e. 1000 times less. In the modern atmosphere, OH is converted into nitric acid on a timescale of about 2 weeks. So, for the early Earth, 1000 times more OH implies a lifetime of (2 weeks/1000) = ~20 min. A typical air parcel in the boundary layer may travel up to 1 km during this time period. We do not consider what occurs before 1% PAL O_2, when the fluxes, and hence OH, were very high and therefore the UV 'protective pockets' must have been very small. We note in passing, however, that volcanoes emit dust and ash which also scatter UV radiation and hence protect the surface – this may also have played a role, especially at the very start of the Proterozoic era.

Conclusions

The results of this work imply that the O_3 smog mechanism has the potential to shield a significant amount of harmful UV radiation from the surface during the Proterozoic era. Owing to positive feedback – in the sense that life produces

https://doi.org/10.1017/S1473550406003478 Published online by Cambridge University Press

some O_2, which then forms some O_3 via the smog mechanism under whose shield more life can propagate, and so on – the mechanism is therefore self-reinforcing.

One may consider, on the other hand, that high levels of tropospheric O_3 protect life from UV radiation but are also toxic to many of today's plants and animals. However, their toxic effect upon early procaryote cells is not well determined.

Many works, for example von Bloh *et al.* (2003), have investigated the 'Pre-Cambrian explosion' characterized by a rapid increase in biomass, occurring at the end of the Proterozoic era. Our results suggest a positive feedback, in which an initial small rise in O_2 levels associated with life leads to tropospheric O_3 production which favours the establishment of more life and so on. We are planning to extend this study using a column model of the early Earth. In a column model, O_3 formed in the upper troposphere would protect the surface from UV radiation and hence slow the smog mechanism. This could lead to lower O_3 columns than the values shown in this sensitivity study.

The results obtained are sensitive to the amount of NO_x assumed, the sources of which are rather uncertain. Our medium value ($=1.53$ ppbv NO_x) runs with 1% PAL O_2 produce a surface ozone mixing ratio of around 1.0×10^{-6}. Assuming this concentration exists throughout the troposphere implies a column value of around double that of the present day (see Appendix B).

Clearly, this result should be checked with a column model to include the effects of self-healing, i.e. ozone increases on the upper levels blocking the passage of UV radiation to lower levels. NO_x values in Table 1 represent global mean averages. However, ambient concentrations of local NO_x may have built up to much higher concentrations in the vicinity of 'hotspots', for example near volcanoes in the early Earth, so the smog mechanism may have evolved in particular locations without requiring large global NO_x averages.

Regarding the anticipated search programs for Earth-like planets, our results point to the possibility of a strong tropospheric O_3 signal in early developing atmospheres, which may be indicated in observations by pressure-broadening effects of spectral lines. Given the large number of young stars in our Solar neighbourhood, the attempt to understand the atmospheric composition of the early Earth is an important focus for the coming decade.

Acknowledgements

We thank the authors of the Master Chemical Mechanism, Leeds University, UK for providing the original chemical scheme.

Appendix A. Overview of the chemical scheme

30 thermal inorganic gas-phase reactions:

$$O + O_2 + N_2 \rightarrow O_3 + N_2$$

$$O + O_2 + O_2 \rightarrow O_3 + O_2$$

$$O + NO \rightarrow NO_2$$

$$O + NO_2 \rightarrow NO + O_2$$

$$O + NO_2 + M \rightarrow NO_3 + M$$

$$O(^1D) + N_2 \rightarrow O + N_2$$

$$O(^1D) + O_2 \rightarrow O + O_2$$

$$NO + O_3 \rightarrow NO_2 + O_2$$

$$NO_2 + O_3 \rightarrow NO_3 + O_2$$

$$NO + NO + O_2 \rightarrow NO_2 + NO_2$$

$$NO + NO_3 \rightarrow NO_2 + NO_2$$

$$NO_2 + NO_3 \rightarrow NO + NO_2 + O_2$$

$$NO_2 + NO_3 + M \rightarrow N_2O_5 + M$$

$$O(^1D) + H_2O \rightarrow OH + OH$$

$$OH + O_3 \rightarrow HO_2 + O_2$$

$$OH + H_2 + O_2 \rightarrow HO_2 + H_2O$$

$$OH + CO + O_2 \rightarrow HO_2 + CO_2$$

$$OH + H_2O_2 \rightarrow HO_2 + H_2O$$

$$HO_2 + O_3 \rightarrow OH + 2O_2$$

$$HO_2 + HO_2 + O_2 \rightarrow H_2O_2 + O_2$$

$$HO_2 + HO_2 + N_2 \rightarrow H_2O_2 + N_2$$

$$OH + NO + M \rightarrow HONO + M$$

$$OH + NO_2 + M \rightarrow HNO_3 + M$$

$$OH + NO_3 \rightarrow HO_2 + NO_2$$

$$HO_2 + NO \rightarrow OH + NO_2$$

$$HO_2 + NO_2 + M \rightarrow HO_2NO_2 + M$$

$$OH + HO_2NO_2 \rightarrow NO_2 + H_2O + O_2$$

$$HO_2 + NO_3 \rightarrow OH + NO_2 + O_2$$

$$OH + HONO \rightarrow NO_2 + H_2O$$

$$OH + HNO_3 \rightarrow NO_3 + H_2O$$

10 inorganic photolysis reactions:

$$O_3 \rightarrow O(^1D) + O_2$$

$$O_3 \rightarrow O + O_2$$

$$H_2O_2 \rightarrow OH + OH$$

$$NO_2 \rightarrow NO + O$$

$$NO_3 \rightarrow NO + O_2$$

$$NO_3 \rightarrow NO_2 + O$$

$$HONO \rightarrow OH + NO$$

$$HNO_3 \rightarrow OH + NO_2$$

https://doi.org/10.1017/S1473550406003478 Published online by Cambridge University Press

Table B1.

Height (km)	Pressure (mb)	T (K)	M (10^{19} molecules cm^{-3})	Column (DU)
0	1013.3	280.0	2.55	80.5
1	877.2	273.5	2.26	71.4
2	759.6	267.0	2.01	63.3
3	657.8	260.5	1.78	56.2
4	569.7	254.0	1.58	49.9
5	493.3	247.5	1.40	44.3
6	427.2	241.0	1.25	39.4
7	369.9	234.5	1.11	35.1
8	320.3	228.0	0.99	31.3
9	277.4	221.5	0.88	27.9
10	240.2	215.0	0.79	24.9
11	208.0	215.0	0.68	21.5
12	180.1	215.0	0.59	18.6
			Total column =	**564.3 DU**

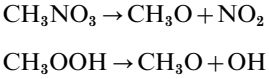

$$CH_3NO_3 \rightarrow CH_3O + NO_2$$

$$CH_3OOH \rightarrow CH_3O + OH$$

15 methane oxidation reactions:

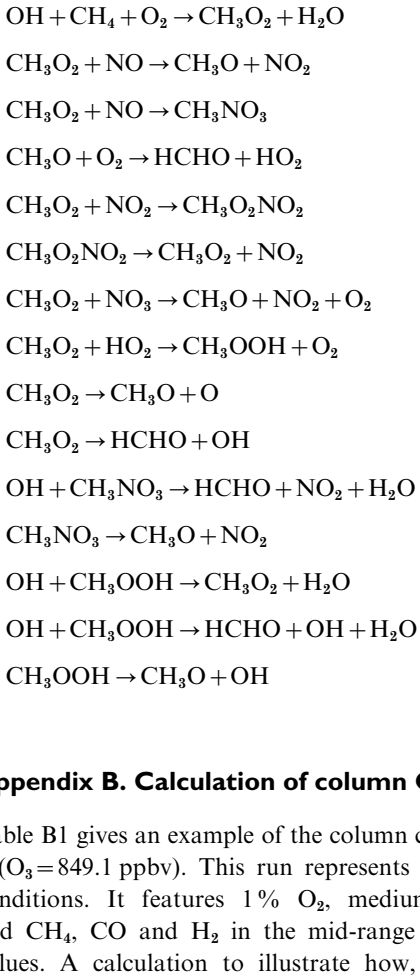

$$OH + CH_4 + O_2 \rightarrow CH_3O_2 + H_2O$$

$$CH_3O_2 + NO \rightarrow CH_3O + NO_2$$

$$CH_3O_2 + NO \rightarrow CH_3NO_3$$

$$CH_3O + O_2 \rightarrow HCHO + HO_2$$

$$CH_3O_2 + NO_2 \rightarrow CH_3O_2NO_2$$

$$CH_3O_2NO_2 \rightarrow CH_3O_2 + NO_2$$

$$CH_3O_2 + NO_3 \rightarrow CH_3O + NO_2 + O_2$$

$$CH_3O_2 + HO_2 \rightarrow CH_3OOH + O_2$$

$$CH_3O_2 \rightarrow CH_3O + O$$

$$CH_3O_2 \rightarrow HCHO + OH$$

$$OH + CH_3NO_3 \rightarrow HCHO + NO_2 + H_2O$$

$$CH_3NO_3 \rightarrow CH_3O + NO_2$$

$$OH + CH_3OOH \rightarrow CH_3O_2 + H_2O$$

$$OH + CH_3OOH \rightarrow HCHO + OH + H_2O$$

$$CH_3OOH \rightarrow CH_3O + OH$$

Appendix B. Calculation of column O_3

Table B1 gives an example of the column calculation for run 9 ($O_3 = 849.1$ ppbv). This run represents mean Proterozoic conditions. It features 1% O_2, medium levels of NO_x and CH_4, CO and H_2 in the mid-range of their reported values. A calculation to illustrate how, for example, we arrived at the value 80.5 DU in the 0–1 km interval then follows. Other values in the table were obtained in a comparable manner.

We took pressure (mb), $P = 1013.3/10^{(z/16)}$, where z = height (km). T (K) was taken from US standard atmosphere (1976). The total number density $(M) = M_{ground} \times (P/P_{ground}) \times (T_{ground}/T)$. Assuming 1 Dobson Unit (DU[4]) $= 2.69 \times 10^{16}$ molecules cm^{-2}, and 1 km thickness Column (DU) $= M \times O_3$ (vmr) $\times$ 100 000 (cm)/DU factor. For example, for $z = 0$ km,

$$2.55 \times 10^{19} \times 849.1 \times 10^{-9} \times 100\,000/(2.69 \times 10^{16})\ \text{DU} = 80.5\ \text{DU}.$$

References

Bada, J.L. (2004). How life began on earth: a status report. *Earth Planet. Sci. Lett.* **226**, 1–15.

Beichman, C.A., Woolf, N.J. & Lindensmith, C.A. (ed.) (1999). The Terrestrial Planet Finder (TPF): a NASA origins program to search for habitable planets. *JPL Publication 99-003*. Available at tpf.jpl.nasa.gov.

Brown, L.L. (1999). Numerical models of reducing primitive atmospheres on Earth and Mars. *PhD Thesis*, Penn State University.

Callis, L.B., Natarajan, M. & Lambeth, J.D. (2001). Solar–atmospheric coupling by electrons (SOLACE). 3. Comparisons and observations, 1979–1997, issues and implications. *J. Geophys. Res.* **106**, 7523–7539.

Cleaves, H.J. & Miller, S.L. (1998). Oceanic protection of prebiotic organic compounds from UV radiation. *Proc. Natl Acad. Sci. USA* **95**, 7260–7263.

Demerjian, K.L., Kerr, J.A. & Calvert, J.G. (1974). The mechanism of photochemical smog. *Adv. Environ. Sci. Technol.* **4**, 1–262.

DeMore, W.B., Sander, S.P., Golden, D.M., Hampson, R.F., Kurylo, M.J., Howard, C.J., Ravishankara, A.R., Kolb, C.E. & Molina, M.J. (1994). Chemical kinetics and photochemical data for use in stratospheric modeling. Evaluation Number 11, JPL Publication, Report no. 94-26. Jet Propulsion Laboratory, Pasadena, CA.

Farquhar, J., Savarino, J., Airieau, S. & Thiemens, M.H. (2001). Observation of wavelength sensitive, mass-independent sulfur isotope effects during SO_2 photolysis: application to the early atmosphere. *J. Geophys. Res.* **106**, 32 829–32 839.

Gear, C.W., Gupta, G.K. & Leimkuhler, B. (1985). Automatic integration of Euler–Lagrange equations with constraints. *J. Comput. Appl. Math.* **12–13**, 77–90.

Grenfell, J.L., Shindell, D.T., Koch, D. & Rind, D. (2001). Chemistry–climate interactions in the Goddard Institute for Space Studies general circulation model: 2. New insights into modeling the preindustrial atmosphere. *J. Geophys. Res.* **106**, 33 435–33 451.

Guinan, E.F. & Ribas, I. (2002). Our changing Sun: the role of solar nuclear evolution and magnetic activity on Earth's atmosphere and climate. In *The Evolving Sun and its Influence on Planetary Environments*, ed. Montesinos, B., Gimenz, A. & Guinan, E.F., pp. 85–107 (*Astronomical Society of the Pacific Conference Series*, vol. 269). Astronomical Society of the Pacific, San Francisco, CA.

Haagen-Smit, A.J. (1951). Chemistry and physiology of Los Angeles Smog. *Indust. Eng. Chem.* **44**, 1342–1346.

Hough, A.M. (1988). The calculation of photolysis rates for use in global tropospheric modelling. Studies. *AERE Report R-13259*, HM Stationery Office, London.

Houghton, J.T., Ding, Y., Griggs, D.J., Noguer, M., van der Linden, P.J., Dai, X., Maskell, K. & Johnson, C.A. (eds.) (2001). Intergovernmental Panel on Climate Change (IPCC), Climate change 2001: the scientific basis. *Contribution of Working Group 1 to the Third Assessment Report*, p. 881. Cambridge University Press, Cambridge.

[4] DU represents a 0.01 mm O_3 column at 0 °C and 1 atm pressure. Typical values are 300–350 DU, i.e. 3–3.5 mm O_3 column at standard temperature and pressure.

https://doi.org/10.1017/S1473550406003478 Published online by Cambridge University Press

Hurtgen, M.T., Arthur, M.A., Suits, N. & Kaufman, A.J. (2002). The sulfur isotopic composition of neoproterozoic seawater sulfate: implications for a snowball earth. *Earth. Planet. Sci. Lett.* **203**, 413–430.

Kasting, J.F. (1993). Earth's early atmosphere. *Science* **259**, 920–926.

Kasting, J.F. (1997). Habitable zones around low mass stars and the search for extraterrestrial life. *Origins Life Evol. Biosphere* **27**, 291–307.

Kasting, J.F. & Catling, D. (2003). Evolution of a habitable planet. *Ann. Rev. Astron. Astrophys.* **41**, 429–463.

Kasting, J.F. & Donahue, T.M. (1980). The evolution of atmospheric ozone. *J. Geophys. Res.* **85**, 3255–3263.

Kerr, R.A. (2005). The story of O_2. *Science* **308**, 1730–1733.

Kumar, P. & Mohan, D. (2002). Photochemical smog mechanism, ill-effects and control. *TERI Information Digest on Energy and Environment* **1(3)**, 445–456.

Lammer, H., Bois, E. & collaborators (2005). Towards real comparative planetology: synergies between solar system science and the DARWIN mission. *39th ESLAB Symposium*, eds Favata, F. & Gimenez, A.

Langematz, U., Grenfell, J.L., Matthes, K., Mieth, P., Kunze, M., Steil, B. & Brühl, C. (2005). Chemical effects in 11-year solar cycle simulations with the Freie Universität Berlin Climate Middle Atmosphere Model with online chemistry (FUB CMAM CHEM). *Geophys. Res. Lett.* **32**, L13803.

Léger, A. (2000). Strategies for remote detection of life – DARWIN-IRSI and TPF Missions. *Adv. Space Res.* **25**, 2209–2223.

Léger, A., Mariotti, J.M., Mennesson, B., Ollivier, M., Puget, J.L., Rouan, D. & Schneider, J. (1996). Could we search for primitive life on extrasolar planets in the near future? The DARWIN project. *J. Astrophys. Space Sci.* **241(1)**, 135–146.

Lenton, T.M., Schellnhuber, H.J. & Szathmáry, E. (2004). Climbing the co-evolution ladder. *Nature* **431**, 913.

Levine, J.S., Hays, P.B. & Walker, J.C.G. (1979). The evolution and variability of atmospheric ozone over geological time. *Icarus* **39(2)**, 295–309.

Mvondo, D.N., Navarro-González, R., McKay, C.P., Coll, P. & Raulin, F. (2001). Production of nitrogen oxides by lightning and coronae discharge in simulated early Earth, Venus and Mars enviroments. *Adv. Space. Res.* **27(2)**, 217–223.

Navarro-González, R., McKay, C.P. & Mvondo, D.N. (2001). Possible nitrogen crisis for Archaean life due to reduced nitrogen fixation by lightning. *Nature* **412**, 61–64.

Pavlov, A.A., Brown, L.L. & Kasting, J.F. (2001). UV shielding of NH_3 and O_2 by organic hazes in the Archaean atmosphere. *J. Geophys. Res.* **106**, 23 267–23 288.

Pavlov, A.A., Hurtgen, M.T., Kasting, J.F. & Arthur, M.A. (2003). Methane-rich proterozoic atmosphere? *Geology* **31(1)**, 87–90.

Pavlov, A.A. & Kasting, J.F. (2002). Mass-independent fractionation of sulfur isotopes in Archaean sediments: strong evidence for an anoxic Archaean atmosphere. *Astrobiology* **2(1)**, 27–41.

Pavlov, A.A., Kasting, J.F. & Brown, L.L. (2000). Greenhouse warming by CH_4 in the atmosphere of early Earth. *J. Geophys. Res.* **105**, 11 981–11 990.

Prather, M. *et al.* (2003). Fresh air in the 21st century? *Geophys. Res. Lett.* **30**, 1100.

Price, C. & Rind, D. (1994). Modelling global lightning distributions in a general circulation model. *Monthly Weather Rev.* **122**, 1930–1939.

Quack, M., Kallenrode, M.B., von König, M., Kümzi, K., Burrows, J., Heber, B. & Wolff, E. (2001). Ground level events and consequences for stratospheric chemistry. *Proceedings of the 27th International Cosmic Ray Conference*, Hamburg, Copernicus Gesellschaft, e.V.

Randall, C.E., Siskind, D.E. & Bevilacqua, R.M. (2001). Stratospheric NO_x enhancements in the southern hemisphere vortex in winter/spring of 2000. *Geophys. Res. Lett.* **28**, 2385–2388.

Ribas, I., Guinan, E.F., Güdel, M. & Audard, M. (2005). Evolution of the solar activity over time and effects on planetary atmospheres: I. High-energy irradiations (1–1700Å). *Astrophys. J.* **622**, 680–694.

Rozanov, E.V., Schlesinger, M.E., Egorova, T.A., Li, B., Andronova, N. & Zubov, V.A. (2004). Atmospheric response to the observed increase of solar UV radiation from solar minimum to solar maximum simulated by the UIUC climate-chemistry model. *J. Geophys. Res.* **109**, D01110.

Rye, R. & Holland, H.D. (1998). Paleosols and the evolution of atmospheric oxygen: a critical review. *Am. J. Sci.* **298**, 621–672.

Rye, R., Kuo, P.H. & Holland, H.D. (1995). Atmospheric carbon dioxide concentrations before 2.2 billion years ago. *Nature* **378**, 603–605.

Sagan, C. & Chyba, C. (1997). The early faint sun paradox: organic shielding of ultraviolet-labile greenhouse gases. *Science* **276**, 1217–1220.

Sagan, C. & Mullen, G. (1972). Earth and Mars: evolution of atmospheres and surface temperatures. *Science* **177**, 52–56.

Schöneberg, R., Kamber, B.S., Collerson, K.D. & Moorbath, S. (2002). Tungston isotope evidence from ~3.8 Gyr metamorphised sediments for early meteorite bombardment of the Earth. *Nature* **418**, 403–405.

Schopf, J.W. (1983). *Earth's Earliest Biosphere: its Origin and Evolution*. Princeton University Press, Princeton, NJ.

Segura, A., Krelove, K., Kasting, J.F., Sommerlatt, D., Meadows, V., Crisp, D., Cohen, M. & Mlawer, E. (2003). Ozone concentrations and ultraviolet fluxes on earth-like planets around other stars. *Astrobiol.* **3**, 689–708.

Selsis, F. (2000). *PhD Thesis*, ch. 5. Universite de Bordeaux. Available at alienor.observ.u-bordeaux.fr/pub/selsis/selsis.pdf.

Selsis, F., Commeyras, A., Dobrijevic, M. & Martin, H. (2002a). Atmospheric levels of NO_x and O_2 on the prebiotic Earth and their possible role in the origin of life. In *Proc. 34th Conf. COSPAR scientific assembly*, Houston, TX, 10–19 October. Elsevier Science.

Selsis, F., Despois, D. & Parisot, J.-P. (2002b). Signature of life on exoplanets: can Darwin produce false positive detections? *Astron. Astrophys.* **388**, 985–1003.

Shindell, D.T., Grenfell, J.L., Rind, D., Grewe, V. & Price, C. (2001). Chemistry–climate interactions in the Goddard Institute for Space Studies general circulation model: 1. Tropospheric chemistry model description and evaluation. *J. Geophys. Res.* **106**, 8047–8076.

Sinnhuber, M., Burrows, J.P., Chipperfield, M.P., Jackman, C.H., Kallenrode, M.B., Künzi, K.F. & Quack, M. (2003). A model study of the impact of magnetic field structure on atmospheric composition during solar proton events. *Geophys. Res. Lett.* **30(15)**, 1818.

Smith, D.S., Scalo, J. & Wheeler, J.C. (2004). Transport of ionizing radiation in terrestrial-like exoplanet atmospheres. *Icarus* **171**, 229–253.

Stamnes, K., Jin, Z., Slusser, J., Booth, C. & Lucas, T. (1992). Several-fold enhancement of biologically effective ultraviolet radiation levels at McMurdo Station, Antarctica during the 1990 ozone 'hole'. *Geophys. Res. Lett.* **19(10)**, 1013–1016.

Thomas, B.C., Melott, A.L., Martin, L.D. & Jackman, C.H. (2004). Ozone abundance in a nitrogen–carbon–dioxide dominated terrestrial paleoatmosphere. *Astrophys. Atmos. Ocean. Phys.* (Geophysical Space Series **10**, 1–7).

Tian, F., Toon, O.B., Pavlov, A.A. & De Sterck, H. (2005). A hydrogen-rich early Earth atmosphere. *Science* **308**, 1014–1017.

von Bloh, W., Bounama, C. & Franck, S. (2003). Cambrian explosion triggered by geosphere–biosphere feedbacks. *Geophys. Res. Lett.* **30(18)**, 1963–1967.

Yienger, J.J. & Levy, H. (1996). Empirical model of global soil-biogenic NO_x emissions. *J. Geophys. Res.* **100(D6)**, 11 447–11 464.